

## LENGTH SCALE IN GRANULAR MEDIA

Matthew R. Kuhn<sup>1</sup> (Member, ASCE) and Takashi Matsushima<sup>2</sup>

### ABSTRACT

The thickness of shear bands depends upon the size of the grains themselves. We consider two possible sources of this scaling: geometric and mechanical. Because each particle occupies space, particle movements are constrained by their physical size and shape and by their surface curvatures at the contacts. We call these origins “geometric.” The motions of each particle are also governed by the mechanics of rigid bodies with compliant contacts. We refer to this origin as “mechanical.” We suggest a general framework for the incremental particle motions of an assembly, accounting for the surface curvatures of particles. We use two-dimensional DEM simulations to test the influence of the mechanical scaling on the shear band thickness. We alter the mechanical scaling by artificially scaling the radii that are used in the kinematic and equilibrium equations. These alterations did not affect shear band thickness. We infer that the thickness has a geometric origin and derives from the sizes, size distribution, and shapes of the particles.

### 1 INTRODUCTION

Localized deformation features are prevalent in granular materials, and the size of a feature often depends upon the sizes of the grains themselves. Shear bands are investigated in this paper, since their thickness is known to depend on particle size. Shear bands can be predicted in a continuum setting, but the continuum model must be enhanced to include some form of an internal length scale. Enhancements to classical continuum models include gradient-dependent constitutive forms, Cosserat type micropolar models, integral type non-local constitutive forms, and visco-plastic models. Although continuum models may produce the localization patterns that are observed in granular, discrete materials, the result is somewhat artificial: key material parameters must be adjusted so that the desired behavior is elicited. These models provide little insight into the underlying mechanisms that produce localization features.

The current study seeks a micro-mechanical rationale for the scale and thickness of shear bands. We have not yet completed the study, but the paper provides our current thoughts about the mechanics of scaling in granular materials. We begin by hypothesizing two possible origins of a length scale in granular materials; we present the results of simulations that test one of the two origins; and then we use the test results to eliminate this origin as a factor in the thickness of shear bands.

---

<sup>1</sup>Dept. of Civil and Env. Engrg., School of Engineering, University of Portland, 5000 N. Willamette, Portland, OR 97203, USA, kuhn@up.edu

<sup>2</sup>Institute of Engineering Mechanics and Systems, University of Tsukuba, 1-1-1, Tennodai, Tsukuba, Ibaraki, 305-8573 Japan, tmatsu@kz.tsukuba.ac.jp

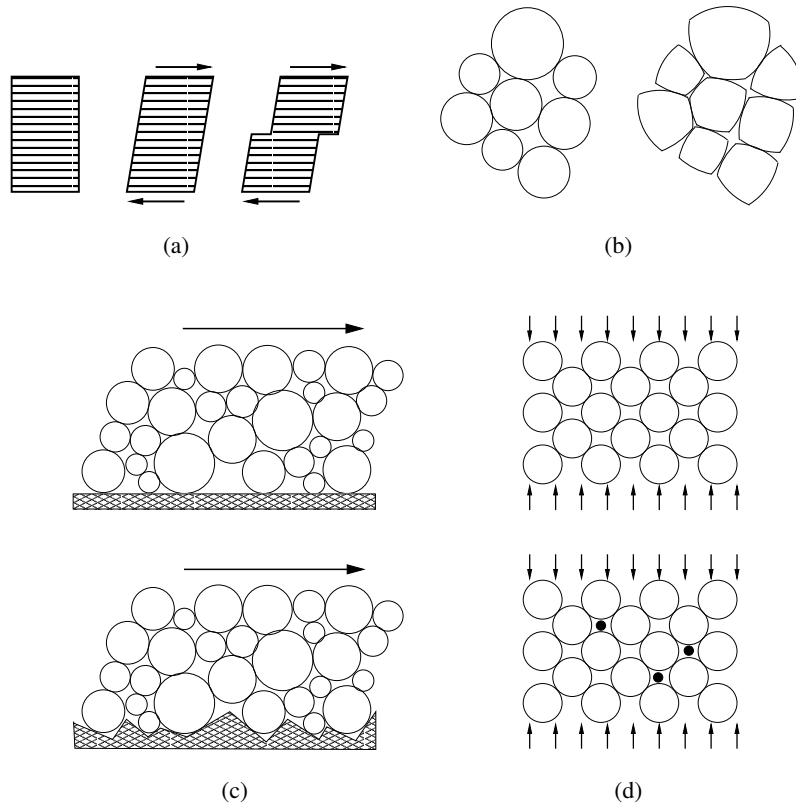


**FIG. 1. Examples of a geometric origin of material behavior.**

## 2 POSSIBLE ORIGINS OF A LENGTH SCALE

Two origins are hypothesized for a length scale in granular materials: geometric and mechanical. Geometric origins are associated with the sizes and shapes of the particles and the consequent interference among particles while an assembly is deformed. Mechanical origins arise from the equilibrium and kinematic equations that apply to individual particles, and to the form of the contact constitutive law. Although the authors have also observed a possible influence of boundary conditions on the emergence and thickness of shear bands, we set aside this influence in the current work.

### 2.1 Geometric origins

Because particles occupy space, their movements are constrained by their physical size, their shapes, and their topological arrangement. We give four examples in which assembly geometry affects material behavior.

- Consider a granular material that is simply a stack of plate-like elastic sheets with a range of inter-sheet frictional characteristics (Fig. 1a). As the assembly is sheared, the stack would, at first, deform uniformly, with each sheet undergoing an equal shearing distortion. Once slipping begins between a single pair of sheets, shearing will continue along the surface between these sheets. The shear band thickness is zero. This thickness is a consequence of the particle shape, the regular arrangement of particles, and the lack

of any rearrangement of sheets during shearing.

- Consider two granular assemblies that share the same topological arrangement of particles, but which have different particle shapes at their contacts (Fig. 1b). Both arrangements may have evolved after an extended phase of initial shearing, but their subsequent incremental behaviors will likely differ, and the shear bands that would eventually appear may also differ in thickness. In Section 2.2, we develop a framework for extracting the influence of particle shape on the incremental material response.
- Consider the interface between a granular material and a wall (Fig. 1c). Incremental deformation near the wall will likely depend on whether the wall is smooth or rough, and the thickness of the interfacial shearing zone may differ for the two conditions.
- Consider the two assemblies in Fig. 1d: the first assembly is entirely regular, but the second assembly contains smaller particles nestled among the larger neighbors. If the two assemblies are compressed, their behaviors will differ, since the larger particles in the second assembly will eventually come into contact with the small particles.

The situation in Fig. 1d resembles mechanisms in shear band evolution. The particles within a shear band are continually rearranged: particles are always coming into contact new neighbors, while existing contacts are always being disengaged. The question of whether a new contact will be created between any two particles depends upon whether they can find each other. This is principally a question of assembly geometry, not of the incremental particle mechanics.

The situations in Figs. 1b and 1d differ in the following respect: the first involves the effect of particle shape on the incremental response; the second involves the changes in assembly topology that result from the particle sizes, shapes, and arrangements.

Although the geometric effects in these examples are somewhat speculative, experiments demonstrate a strong influence of particle shape and arrangement on shear band thickness. O’Sullivan and Bray (2003) tested carefully constructed, regular packings of equal-size metal balls and observed shear bands that were much thinner than those usually observed in irregular packings. Yoshida and Tatsuoka (1997) placed metal balls in a regular arrangement between two glass plates and observed the deformations during biaxial (2D) loading. They found that the shear band had a thickness of three balls, which is also much thinner than shear bands typically observed in irregular packings. The conditions in these tests—regular particle arrangements with no rearrangement of the assembly topology—are similar to those of the first example. Bagi (2003) and Babic et al. (1990) have also demonstrated an effect of assembly regularity on the size of localization phenomena, and Bagi has proposed measures for quantifying the notion of “regularity” in granular materials. In contrast, Viggiani et al. (2001) found that the thickness of shear bands in sand specimens depended on the mean grain size but not on the size distribution.

## 2.2 Mechanical origins

Incremental particle motions are governed by the mechanics of rigid bodies with compliant contacts: particle motions produce contact deformations; contact deformations produce contact forces; and the contact forces on each particle must be in equilibrium. Each of these three relations introduces a length scale.

Particles  $p$  and  $q$  are in contact at the point  $c$  (Fig. 2). The contact forces  $\mathbf{f}$  on a particle must be in equilibrium:

$$\sum_q \mathbf{f}^{pq} = \mathbf{b}, \quad \sum_q \mathbf{r}^{pq} \times \mathbf{f}^{pq} = \mathbf{m}, \quad (1)$$

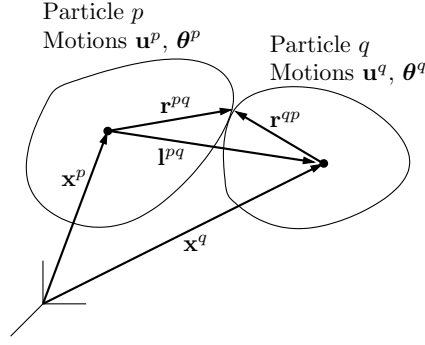


**FIG. 2. Two particles in contact.**

where the sums are over all particles “ $q$ ” that are in contact with  $p$ , and  $\mathbf{b}$  and  $\mathbf{m}$  are the body force and moment on  $p$ . The radial vectors  $\mathbf{r}^{pq}$  are directed from a single reference point on  $p$  to its contact with  $q$ . Equation (1<sub>2</sub>) includes an intrinsic length—the radius  $\mathbf{r}^{pq}$ . We will later test the scaling of shear band phenomena by running simulations with entirely *contrived* mechanical radii  $\alpha r_i^{pq}$  instead of the real radii  $r_i^{pq}$  in the moment equilibrium equation  $[\mathbf{A}_2][\delta\mathbf{f}]$ .

The increment of a contact force  $\delta\mathbf{f}^{pq}$  depends upon the contact deformation, perhaps in the form

$$\delta\mathbf{f}^{pq} = F^{pq}(\delta\mathbf{u}^{pq, \text{def}}, \mathbf{f}^{pq}) \cdot \delta\mathbf{u}^{pq, \text{def}}. \quad (2)$$

We have excluded viscous effects in this form (see Pöschel et al. 2001), along with any effect of the contact history, but we allow the incremental response to depend on the current contact force  $\mathbf{f}^{pq}$ , as would apply with frictional contacts. The constitutive form (2) is incrementally non-linear, as would be expected for frictional contacts. The choice of a contact law  $F^{pq}(\cdot)$  will affect material scaling, and in Section 3, we give the results of numerical, DEM simulations in which a simple, linear contact law is altered by selecting different contact friction coefficients. We then determine the effect, if any, on shear band thickness.

The contact deformation  $\delta\mathbf{u}^{pq, \text{def}}$  depends upon the particle motions,

$$\delta\mathbf{u}^{pq, \text{def}} = d\mathbf{u}^q - d\mathbf{u}^p + (d\boldsymbol{\theta}^q \times \mathbf{r}^{qp} - d\boldsymbol{\theta}^p \times \mathbf{r}^{pq}), \quad (3)$$

where  $d\mathbf{u}^p$  and  $d\mathbf{u}^q$  are the incremental displacements of the two particles, and  $d\boldsymbol{\theta}^p$  and  $d\boldsymbol{\theta}^q$  are their incremental rotations. Equation (3) contains the components  $r_i^{pq}$  of particle radii. We consider these radii as being “mechanical radii,” since they are associated with the kinematics of particle interaction. We will later test the scaling of shear band phenomena by running simulations with contrived radii  $\beta r_i^{pq}$  in place of the real radii  $r_i^{pq}$ .

Equations (1), (2), and (3) can be gathered into a matrix stiffness equation for all  $N$  particles of an assembly:

$$[\mathbf{H}]_{6N \times 6N} \begin{bmatrix} d\mathbf{u} \\ d\boldsymbol{\theta} \end{bmatrix}_{6N \times 1} = [\mathbf{c}]_{6N \times 1} \quad (4)$$

where  $[\mathbf{H}]$  is the stiffness matrix,  $[\mathbf{c}]$  is the forcing vector, and vector  $[d\mathbf{u}/d\boldsymbol{\theta}]$  contains the displacements and rotations of all  $N$  particles. By considering the incremental form of Eq. (1), we can expand Eq. (4) as follows:

$$\left( [\mathbf{A}_1] + [\mathbf{A}_2][\mathbf{A}_3] + [\mathbf{A}_2] \left[ \mathbf{F}([\delta\mathbf{u}^{\text{def}}], [\mathbf{f}]) \right] [\mathbf{B}] \right) \begin{bmatrix} d\mathbf{u} \\ d\boldsymbol{\theta} \end{bmatrix} = [\mathbf{c}]. \quad (5)$$

**TABLE 1. Test conditions for DEM simulations.**

Test No.	Static	Kinematic	Friction $\mu$
	length factor $\alpha$	length factor $\beta$	
1	1.0	1.0	0.5
2	0.5	2.0	0.5
3	1.0	0.5	0.5
4	0.5	0.5	0.5
5	2.0	2.0	0.5
6	1.0	1.0	0.25
7	1.0	1.0	1.0

Although it is difficult to entirely separate geometric and mechanical effects, we would say that the stiffnesses  $[\mathbf{A}_1]_{6N \times 6N}$  and  $[\mathbf{A}_3]_{3M \times 6N}$  are geometric in origin: they include the products of the particle radii, the surface curvatures of the particles at their  $M$  contacts points, and the cumulative contact forces. Matrices  $[\mathbf{A}_2]_{6N \times 3M}$ ,  $[\mathbf{F}]_{3M \times 3M}$ , and  $[\mathbf{B}]_{3M \times 6N}$  are mechanical in origin:  $[\mathbf{A}_2]$  is the statics matrix;  $[\mathbf{F}]$  is the contact stiffness matrix; and  $[\mathbf{B}]$  is the assembly kinematics matrix. In the next section we use simulations to explore the effect of altering the length scales within the mechanical stiffness, while leaving the geometric stiffness unchanged.

### 3 SIMULATIONS

Several DEM shearing simulations were conducted with altered mechanical radii and with different coefficients of contact friction, and we compare the thicknesses of the shear bands that appeared in these simulations. The mechanical radii were altered with five combinations of the factors  $\alpha$  and  $\beta$ : the static factor  $\alpha$  was multiplied by the radii that appear in the moment equilibrium Eq. (1<sub>2</sub>), and the kinematic factor  $\beta$  was multiplied by the radii within the kinematic Eq. (3). Five combinations of factors  $\alpha$  and  $\beta$  were applied in the five simulations, but within each simulation, the same pair of values was used with all particles (Tests 1–5, Table 1). Contact detection was based entirely upon the actual, geometric radii, so that a mechanical origin of material scaling could be distinguished from a geometric origin. That is, the contact detection process assured that particles would roll across their geometric surfaces, and that contact formation and disengagement would also conform to the actual geometric shapes. Another three tests were conducted with the same  $\alpha = \beta = 1$  but with different contact friction coefficients  $\mu$  (Tests 1, 6, and 7, Table 1). The purpose of these three tests was to distinguish any constitutive-mechanical origin of the material scale.

Other than modifying the mechanical radii, the Discrete Element Method (DEM) was implemented in a conventional manner. The DEM algorithm uses dynamic relaxation to resolve the equilibrium, kinematic, and constitutive equations, rather than the matrix approach outlined in Section 2.2. The DEM algorithm is simply an efficient approach for the solving the same set of (incrementally non-linear) equations. The meaning of the mechanical scaling factors may be more clearly understood in the context of the DEM algorithm, particularly when applied to circular disks. With an  $\alpha = 0$ , no particle rotations will occur, since any moment imbalances that would be produced by tangential forces are nullified by the  $\alpha$  and will not impel particle rotations. With a  $\beta = 0$ , particle rotations produce no tangential contact forces.

The rectangular assembly contained 40,050 unbonded circular disks of multiple diameters. The disk sizes were randomly distributed over a fairly narrow range of between  $0.56\bar{D}$  and  $1.7\bar{D}$ , where  $\bar{D}$  is the mean particle diameter. The assembly was created by slowly and

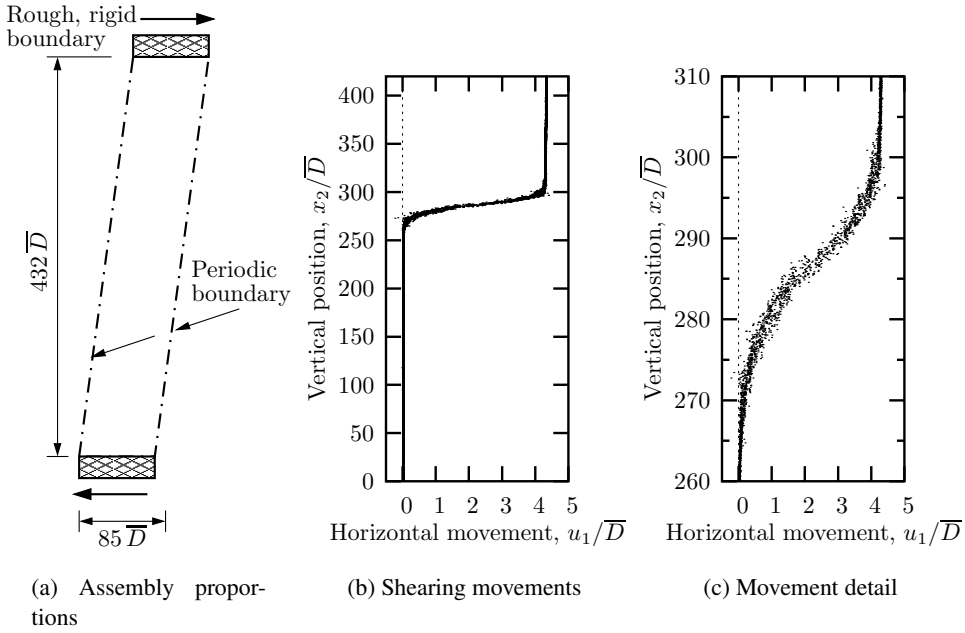


**FIG. 3. The assembly of 40,050 circular disks and the observed shearing displacements.**

isotropically compacting a sparse arrangement of particles within a set of periodic boundaries that surrounded the assembly. During compaction, the friction between particles was disallowed (although friction was later restored for the shearing tests). This technique produced a material that was dense, random, and isotropic, at least when viewed at a macro-scale. The average initial void ratio was 0.1730 (solid fraction of 0.8525), the initial average coordination number was 3.93, and the average overlap between neighboring particles was about  $4 \times 10^{-4}$  of  $\bar{D}$ . Contact stiffness was in the form of normal and tangential springs of equal stiffness.

After compaction, the periodic boundaries were removed from the top and bottom of the assembly and were replaced with rough rigid platens. These platens were simply thin layers of tightly intermeshed particles that were placed by shifting a (periodic) subset of particles onto the top and bottom of the assembly. The final assembly was  $84\bar{D}$  wide and  $432\bar{D}$  tall (Fig. 3a).

The assembly was horizontally sheared in all of the tests. Vertical dilation was freely allowed by maintaining a constant vertical stress throughout the shearing process, but the assembly width was maintained constant. These conditions are similar to those employed by Cundall (1989) and Matsushima et al. (2003). Shear bands developed in all of the simulations, regardless of the choices of  $\alpha$ ,  $\beta$ , and  $\mu$ . An example is shown in Figs. 3b–c, which plot the horizontal particle movements  $u_1^p$  of all 40,050 particles as a function of their vertical positions  $x_2^p$  ( $\alpha = \beta = 1$ ,  $\mu = 0.5$ ). The plots show the horizontal displacements that had occurred between the shearing strains of 9% and 10%. All movements and positions are expressed in a dimensionless form by dividing by the mean (geometric) diameter  $\bar{D}$ . Plots of the shearing stress are shown in Fig. 4 for each of the friction coefficients ( $\mu = 0.25, 0.5$ , and  $1.0$ ,  $\alpha = \beta = 1$ ). Although the peak strength increases with an increasing friction coefficient, the residual strength is independent of  $\mu$ .

The primary question is whether a mechanical scaling of radii by the factors  $\alpha$  and  $\beta$  will

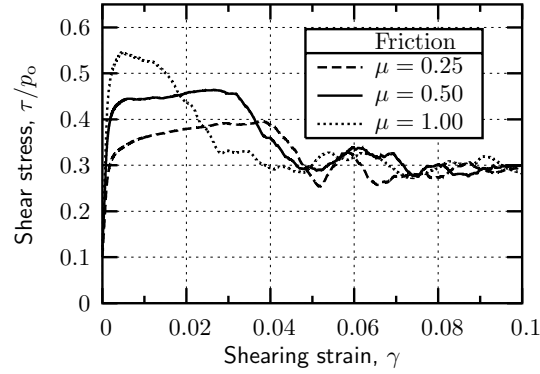
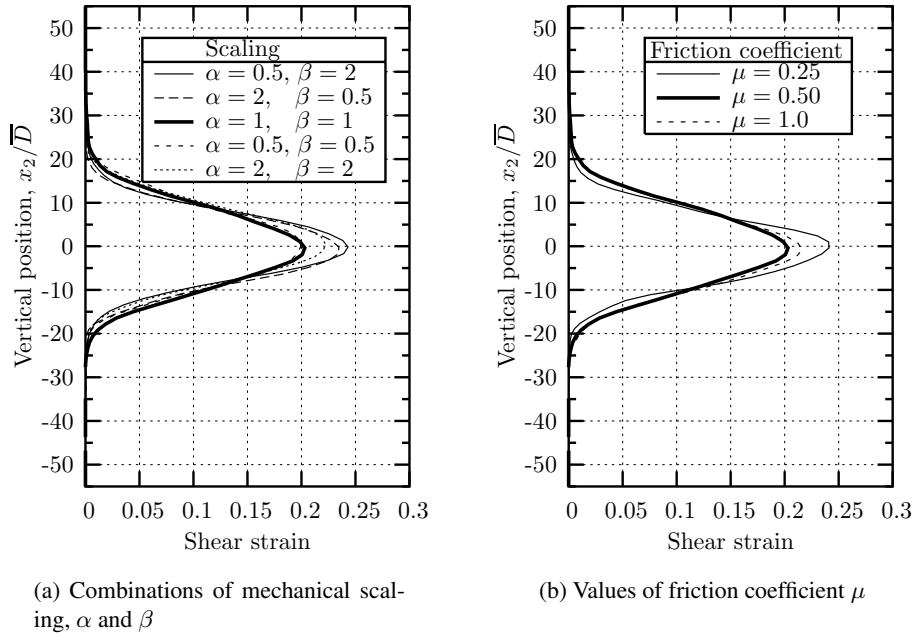


FIG. 4. Evolution of shear stress for three friction coefficients.



(a) Combinations of mechanical scaling,  $\alpha$  and  $\beta$

(b) Values of friction coefficient  $\mu$

FIG. 5. Shear strain profiles with shear bands for various combinations of  $\alpha$ ,  $\beta$ , and  $\mu$ .

affect shear band thickness. The factors  $\alpha$  and  $\beta$  have no effect on thickness. Figure 5a shows the smoothed profiles of shearing strain within the shear bands for five simulations having different combinations of  $\alpha$  and  $\beta$ . The strain profiles have been centered at mid-thickness of the bands, even though shear bands appeared at different heights in the five tests. The five bands share the same thickness and almost identical strain profiles. The friction coefficient  $\mu$  also has not effect on shear band thickness, as is shown in Fig. 5b.

#### 4 CONCLUSION

The simulation results were surprising. We had expected some effect of mechanical scaling on shear band thickness, but the thicknesses were the same for all values of mechanical scaling,  $\alpha$  and  $\beta$ , and for all friction coefficients  $\mu$ . Shear band thickness seems to have a geometric

origin and to depend upon the geometric sizes, size distribution, and shape of the particles, although this conclusion will need to be confirmed with additional tests. We have already noted that regular packings of equal-size spheres and disks exhibit shear bands that are much thinner than those of the current study (Babic et al. 1990; O’Sullivan and Bray 2003; Bagi 2003). We plan to conduct 2D tests with different distributions of disk sizes (similar to the physical experiments of Viggiani et al. 2001) and with oval shapes having different aspect ratios.

## REFERENCES

- Babic, M., Shen, H. H., and Shen, H. T. (1990). “The stress tensor in granular shear flows of uniform, deformable disks at high solids concentrations.” *J. Fluid Mech.*, ASME, 219(10), 81–118.
- Bagi, K. (2003). “From order to chaos: the mechanical behavior of regular and irregular assemblies.” *Quasi-Static Deformations of Particulate Materials*, K. Bagi, ed., Proc. of the QuaDPM’03 Workshop, Aug. 25–28, Budapest, Hungary. 151–158.
- Cundall, P. (1989). “Numerical experiments on localization in frictional materials.” *Ingenieur-Archiv*, 59(2), 148–159.
- Matsushima, T., Saomoto, H., Tsubokawa, Y., and Yamada, Y. (2003). “Observation of grain rotation inside granular assembly during shear deformation.” *Soils and Found.*, 43(4), 95–106.
- O’Sullivan, C. and Bray, J. D. (2003). “Evolution of localization in idealized granular materials.” *Quasi-Static Deformations of Particulate Materials*, K. Bagi, ed., Proc. of the QuaDPM’03 Workshop, Aug. 25–28, Budapest, Hungary. 151–158.
- Pöschel, T., Salueña, C., and Schwager, T. (2001). “Scaling properties of granular materials.” *Continuous and Discontinuous Modelling of Cohesive-Frictional Materials*, P. A. Vermeer, S. Diebels, W. Ehlers, H. J. Herrmann, S. Luding, and E. Ramm, eds., Springer, Berlin, 174–184.
- Viggiani, G., Küntz, M., and Desrues, J. (2001). “An experimental investigation of the relationships between grain size distribution and shear banding in sand.” *Continuous and Discontinuous Modelling of Cohesive-Frictional Materials*, P. A. Vermeer, S. Diebels, W. Ehlers, H. J. Herrmann, S. Luding, and E. Ramm, eds., Springer, Berlin, 111–127.
- Yoshida, T. and Tatsuoka, F. (1997). “Deformation property of shear band in sand subjected to plane strain compression and its relation to particle characteristics.” *Proc. 14th Int. Conf. Soil Mech. and Found. Engrg., Hamburg*, Vol. 1, 237–240.